

HIGH BANDWIDTH CONTROL OF A PIEZOELECTRIC STAGE IN THE PRESENCE OF RATE-DEPENDENT HYSTERESIS

Jinhao Chen

Dept. of Mechanical Engineering
Texas Tech University
Lubbock, Texas 79409
Email: jinhao.chen@ttu.edu

Beibei Ren

Dept. of Mechanical Engineering
Texas Tech University
Lubbock, Texas 79409
Email: beibei.ren@ttu.edu

Qing-Chang Zhong

Dept. of Electrical and
Computer Engineering
Illinois Institute of Technology
Chicago, Illinois 60616
Email: zhongqc@ieee.org

INTRODUCTION

Piezoelectric nanopositioning actuators are widely employed in many applications, including the hard disk drives [1–3], gyroscopes [4] and the scanning probe microscopes [5]. Besides the precise position control, high-bandwidth tracking control is crucial for the applications of piezoelectric actuators, since, for example, it will allow hard disk drives to meet the demand for higher data storage capacities with lower access times [6]. However, the existence of vibration dynamics, the coupled hysteresis and other uncertainty (e.g. creep) greatly limit the positioning and tracking performance of the piezoelectric actuators over a broad bandwidth. As a solution to tackle this problem and achieve precise control over a broad frequency range, stiffer piezoelectric actuators that have higher resonant frequencies can be employed. In this way, the scan frequency at which the vibration is significant becomes higher, while, as a major disadvantage, the range of motion is reduced [7]. This highly motivates the development of control techniques that enable high-bandwidth nanopositioning of piezoelectric-actuated systems.

In order to perform the high-bandwidth high-precision tracking on the piezoelectric-actuated systems, numerous controllers have been developed based on a cascade model of the rate-independent hysteresis and vibration dynamics [5, 8]. Different from these work, the input-output relation of the piezoelectric stage can be also considered as a rate-dependent hysteresis model [9]. In this paper, to achieve the high-bandwidth control on a piezoelectric stage, the rate-dependent hysteresis is reconstructed as a linear function plus an unknown nonlinear term.

Then, in order to estimate and compensate such an unknown nonlinear term together with other uncertainties, the uncertainty-and-disturbance-estimator (UDE)-based controller will be further developed based on the internal model principle [10]. Experimental results will be provided to show that the proposed UDE-based controller can well achieve high-bandwidth precise control.

EXPERIMENTAL SETUP AND SYSTEM CHARACTERIZATION

The experimental setup is shown in Fig. 1. The detailed specification of the piezoelectric nanopositioning system can be referred to <http://www.pi.ws>. The sampling frequency is chosen as $40kHz$.

In order to show that the hysteresis in piezoelectric stage is indeed rate-dependent, three sinusoidal signals in the form of $v(t) = 3(\sin(2\pi ft) + 1)$ with the frequencies $f = 1Hz, 50Hz, 100Hz$ are used as the excitation to obtain a series of major hysteresis loops, which are shown in Fig. 2(a). It can

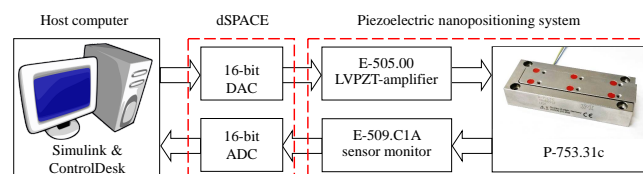


FIGURE 1. Experimental setup of P-753.31c nanopositioning system.

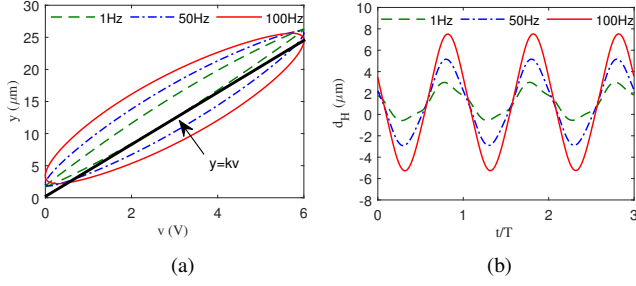


FIGURE 2. (a) Major hysteresis loops of P-753.31c excited by sinusoidal signals with different frequencies, (b) Nonlinear uncertain term $d_H = H[v](t) - kv(t)$.

be clearly seen that the hysteresis between the input voltage $v(t)$ and the output displacement $y(t) = H[v](t) + d(t)$ exhibits a rate-dependent effect with the increase of the frequency of the input, where $d(t)$ includes some unknown bounded disturbances and uncertainties (e.g., creep effect and modeling error). To compensate the rate-dependent hysteresis $H[v](t)$, it will firstly be constructed as a linear function plus the unknown nonlinear term $d_H(t) = H[v](t) - kv(t)$ in this paper, i.e.,

$$H[v](t) = kv(t) + d_H(t), \quad (1)$$

where k should be chosen as the slope of the asymptotes of the hysteresis loops to ensure the boundedness of d_H [8] as illustrated in Fig. 2(a). The resulted nonlinear term d_H when $k = 4.33$ is shown in Fig. 2(b), where the horizontal axis is scaled by the periods of the signals.

CONTROLLER DESIGN

To facilitate the controller design, a filter will be added on the output $y(t)$ to generate the filtered output $x(t)$. For simplification, a first-order low-pass filter is adopted, which can be also replaced by other higher-order low-pass filters, then

$$x(t) = \mathcal{L}^{-1} \left\{ \frac{\rho}{s + \rho} \right\} * (H[v](t) + d(t)), \quad (2)$$

where “*” is the convolution operator, $\mathcal{L}^{-1}\{\cdot\}$ is the operator of inverse Laplace transform. By choosing a proper value of $\rho > 0$, it holds that $x(t) \approx y(t)$. Based on (1) and (2), the dynamics of the piezoelectric stage is rewritten as

$$\begin{aligned} \dot{x}(t) &= -\rho x(t) + \rho H[v](t) + \rho d(t) \\ &= -\rho x(t) + \rho kv(t) + u_d(t), \end{aligned} \quad (3)$$

with $u_d(t) \triangleq \rho d_H(t) + \rho d(t)$.

For the required specifications of the closed-loop system, the following stable reference model ($A_m > 0$) can be chosen with the piecewise continuous and uniformly bounded command $c(t)$

$$\dot{x}_m(t) = -A_m x_m(t) + B_m c(t). \quad (4)$$

The control objective is to design a control signal $v(t)$ such that, for any desired continuous trajectory $x_m(t)$, the tracking error defined as $e(t) = x_m(t) - x(t)$ asymptotically converges to zero. The desired error dynamics governed by $\dot{e}(t) = -Ke(t)$, where $K > 0$ is the error feedback gain. From (3), there is $u_d(t) = \dot{x}(t) + \rho x(t) - \rho kv(t)$. By using the UDE [8], $u_d(t)$ can be estimated as

$$\hat{u}_d(t) = g_f(t) * u_d(t) = g_f(t) * (\dot{x}(t) + \rho x(t) - \rho kv(t)) \quad (5)$$

where $g_f(t)$ is the impulse response of a low-pass filter $G_f(s)$, which should be stable and strictly proper, and have the unity gain and zero phase shift over the spectrum of $u_d(t)$ and zero gain elsewhere. According to the filter design based on the internal model principle [10], the filter $G_f(s)$ is chosen as follows

$$G_f(s) = 1 - \frac{s(s^2 + \omega^2)}{(s + \alpha)(s^2 + \alpha_1 s + \beta_1)}, \quad (6)$$

where $\omega = 2\pi f$, and α , α_1 and β_1 are design parameters. By combining (3), (4) and the desired error dynamics, there is

$$-Ke(t) = -A_m x_m + B_m c + \rho x(t) - \rho kv(t) - u_d(t). \quad (7)$$

By replacing $u_d(t)$ in (7) with $\hat{u}_d(t)$ in (5), the UDE-based controller can be obtained as

$$\begin{aligned} v(t) &= \frac{1}{\rho k} \left[\rho x(t) - \mathcal{L}^{-1} \left\{ \frac{s G_f(s)}{1 - G_f(s)} \right\} * x(t) \right. \\ &\quad \left. + \mathcal{L}^{-1} \left\{ \frac{1}{1 - G_f(s)} \right\} * (-A_m x_m + B_m c + Ke(t)) \right]. \end{aligned} \quad (8)$$

EXPERIMENTAL RESULTS

To verify the effectiveness of the UDE-based controller (8) with the filter $G_f(s)$ in (6) is implemented on the experimental setup illustrated in Fig. 1 to track the desired trajectory $x_m(t)$ in (4) with $c(t) = A(\sin(2\pi f t - \pi/2) + 1)$. The parameters are chosen in the following manner. First, A_m and B_m are set as 80000

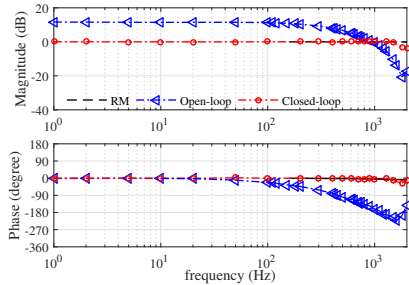


FIGURE 3. Bode plots of the reference model (RM), the open-loop system and the closed-loop system.

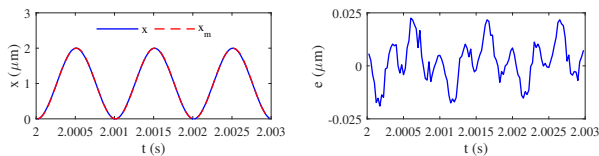


FIGURE 4. Tracking results for $f = 1000\text{Hz}$: position $x(t)$ and tracking error $e(t)$.

to ensure that the bandwidth of the reference model (4) satisfies the desired performance of the closed-loop system. Then, the parameter ρ in (2) is chosen such that the bandwidth of the filter is at least 10 times of the tracking signal, which results in $\rho = \min(20\pi f, 80000)$. For the error feedback gain, a larger K can increase the rate of convergence of the tracking error but, on the other hand, the instability may be resulted in if K is too large. In this experiment, $K = 800$. Finally, the parameters for $G_f(s)$ in (6) are chosen as $\alpha = 1000$, $\alpha_1 = \min(4\pi f, 4\pi \times 450)$, and $\beta_1 = \min(8\pi^2 f^2, 8\pi^2 \times 450^2)$. As recommended by the manufacturer, the highest tracking frequency is 2kHz .

The Bode plots of the reference model (4), the open-loop system and the closed-loop system are shown in Fig. 3, whose transfer functions are $X_m(s)/C(s)$, $X(s)/V(s)$, and $X(s)/C(s)$, respectively. It can be seen that the closed-loop system with the UDE-based controller can well track the reference signal up to 1500Hz , which is much higher than the bandwidth achieved by the robust adaptive controller [11] on the same platform. The tracking results for $f = 1000\text{Hz}$ and $A = 1\mu\text{m}$ are provided in Fig. 4. It can be seen that the maximum tracking error is $0.0225\mu\text{m}$, i.e., 1.12% of the travel range of the reference signal, which is close to the maximum relative error $0.0864/7.6 = 1.14\%$ for $f = 100\text{Hz}$ using the robust adaptive controller [11].

CONCLUSION

In this paper, the rate-dependent hysteresis in a piezoelectric stage is firstly reconstructed as a linear term plus an unknown nonlinear term. The unknown term together with other uncertainties are then estimated and compensated by the UDE-based

controller that is developed based on the internal model principle. Experimental results had been provided to show that the desired trajectory in a wide range of frequency can be accurately tracked by the proposed UDE-based controller.

REFERENCES

- [1] Shahsavari, B., Keikha, E., Zhang, F., and Horowitz, R., 2015. "Adaptive repetitive control design with online secondary path modeling and application to bit-patterned media recording". *IEEE Trans. Magn.*, **51**(4), pp. 1–8.
- [2] Shahsavari, B., Conway, R., Keikha, E., Zhang, F., and Horowitz, R., 2013. "Robust track-following controller design for hard disk drives with irregular sampling". *IEEE Trans. Magn.*, **49**(6), pp. 2798–2804.
- [3] Xi, W., and Zhang, W., 2015. Data storage device compensating for hysteretic response of microactuator, Oct. 6. US Patent 9 153 283.
- [4] Zhang, F., Keikha, E., Shahsavari, B., and Horowitz, R., 2014. "Adaptive mismatch compensation for rate integrating vibratory gyroscopes with improved convergence rate". In ASME 2014 Dynamic Systems and Control Conference, American Society of Mechanical Engineers, p. V003T45A003.
- [5] Clayton, G. M., Tien, S., Leang, K. K., Zou, Q., and Devasia, S., 2009. "A review of feedforward control approaches in nanopositioning for high-speed SPM". *J. Dyn. Syst., Meas. Control*, **131**(6), p. 061101.
- [6] Wernow, J., and Horowitz, R., 2012. "Quasi-shear mode piezoelectric microactuator for head-based servo control in hard disk drives". In Micro Electro Mechanical Systems (MEMS), 2012 IEEE 25th International Conference on, IEEE, pp. 1169–1172.
- [7] Yan, G., Liu, Y., and Feng, Z. H., 2015. "A dual-stage piezoelectric stack for high-speed and long-range actuation". *IEEE/ASME Trans. Mechatronics*, **20**(5), pp. 2637–2641.
- [8] Chen, J., Ren, B., and Zhong, Q.-C., 2016. "UDE-based trajectory tracking control of piezoelectric stages". *IEEE Trans. Ind. Electron.* accepted.
- [9] Al Janaideh, M., and Krejci, P., 2013. "Inverse rate-dependent Prandtl–Ishlinskii model for feedforward compensation of hysteresis in a piezomicropositioning actuator". *IEEE/ASME Trans. Mechatronics*, **18**(5), pp. 1498–1507.
- [10] Ren, B., Zhong, Q.-C., and Dai, J., 2016. "Asymptotic reference tracking and disturbance rejection of UDE-based robust control". submitted.
- [11] Gu, G.-Y., Zhu, L.-M., Su, C.-Y., and Ding, H., 2013. "Motion control of piezoelectric positioning stages: modeling, controller design, and experimental evaluation". *IEEE/ASME Trans. Mechatronics*, **18**(5), pp. 1459–1471.